

# About the Stability of Active Queue Management Mechanisms

Dario Bauso, Laura Giarré and Giovanni Neglia

**Abstract**—In this paper, we discuss the influence of multiple bottlenecks on the stability of Active Queue Management (AQM) controllers, usually configured on a single bottleneck basis. To see this, we consider a network scenario where RED is configured at each router according to previously developed control theoretic techniques. These configuration rules assure stability in a single bottleneck scenario. Yet, we show that instability may arise when two links become congested. We justify this result through a multiple bottleneck model.

## I. INTRODUCTION

AQM has been proposed to support end-to-end TCP congestion control in the Internet [1]. AQM controllers operate at the network nodes to detect incipient congestion and indicate it to TCP sources, which reduce their transmission rate in order to prevent worse congestion. Usually packet drops are used for congestion indication.

Many AQM schemes have been proposed [2], [3], [4], [5], whose algorithms usually rely on some heuristics and their performances appear to be highly dependant on the considered network scenario (see, e.g., [6], [7], [8], as regards the well-known Random Early Detection -RED- algorithm).

This paper is motivated by the consideration that the distributed fashion of TCP flows control across the network has not been explicitly considered up to now. As a matter of fact TCP flows may turn to be controlled at the same time by two or more nodes acting independently according to their AQM settings. According to our opinion, this can hardly affect AQM algorithms performance. In particular, we propose a counterexample to show that RED controllers, configured according to [9], do not prevent from instability if two nodes face congestion at the same time (this is referred to as *multiple bottleneck scenario*).

This paper is organized as follows. Section II recollects some results from [9], which will be referred to in the following sections. In Section III we present a multiple bottleneck network scenario, that exhibits instability. The presence of instability is derived from performance metrics obtained through simulations. In Section IV, we provide an analytical insight to better understand the experimental results. Finally, conclusive remarks and further research issues are given in Section V. In particular we discuss the development of new cooperative congestion local controllers under the assumption that a congested node may communicate its state to the neighbors.

D. Bauso is with DINFO, Università di Palermo, 90128 Palermo, Italy [bauso@ias.unipa.it](mailto:bauso@ias.unipa.it)

L. Giarré is with DIAS, Università di Palermo, 90128 Palermo, Italy [giarre@unipa.it](mailto:giarre@unipa.it)

G. Neglia is with DIE, Università di Palermo, 90128 Palermo, Italy [giovanni.neglia@tti.unipa.it](mailto:giovanni.neglia@tti.unipa.it)

## II. SINGLE BOTTLENECK MODEL

The starting point in [9] is the model described by the following coupled, nonlinear differential equations:

$$\dot{W}(t) = \frac{1}{R(t)} - \frac{W(t)W(t-R(t))}{2R(t-R(t))}p(t-R(t)) \quad (1)$$

$$\dot{q}(t) = \frac{W(t)}{R(t)}N(t) - 1_{q(t)}C \quad (2)$$

where  $1_q = 1$  if  $q > 0$ ,  $1_q = 0$  otherwise. Symbols used in the equations above are summarized in the following table.

$W$	expected TCP window size (packets);
$q$	expected queue length (packets);
$R$	round-trip time;
$C$	link capacity (packets/sec);
$T_p$	propagation delay (secs);
$N$	load factor (number of TCP sessions);
$p$	probability of packet drop;

The first equation represents the TCP window, that increases by one every round trip time, and halves when a packet loss occurs. Packet loss rate is computed as the dropping probability times the number of packets sent per time unit. The round trip time is related to the propagation delay and the queue occupancy by the following relation:  $R = T_p + \frac{q}{C}$ . The second equation represents the variation of queue occupancy as the difference between the input traffic and the link capacity.

AQM schemes determine the relation between the dropping probability and the nodes congestion status.

Here we considered RED as AQM scheme. RED configuration is specified through four parameters: the minimum and the maximum threshold ( $THR_{min}$ ,  $THR_{max}$ ), the maximum dropping probability in the region of random discard  $P_{max}$ , and the weight coefficient  $w_q$ . RED can be modelled by the following equations (refer to [2] for RED operation):

$$\begin{aligned} \dot{x}(t) &= -Kx(t) + Kq(t) & (3) \\ p(x) &= \begin{cases} 0, & 0 \leq x < THR_{min} \\ \frac{(x-THR_{min})P_{max}}{THR_{max}-THR_{min}}, & THR_{min} \leq x < THR_{max} \\ 1, & THR_{max} \leq x, \end{cases} & (4) \end{aligned}$$

where  $K = -\ln(1-\alpha)/\delta$  and  $\delta$  is the time between two queue samples. The time interval  $\delta$  can be assumed to be equal to  $1/C$  for a congested node.

The linearized system (TCP sources, congested node queue and AQM controller) can be represented by the block diagram of Figure 1. In the block diagram  $L = P_{max}/(THR_{max} - THR_{min})$ .

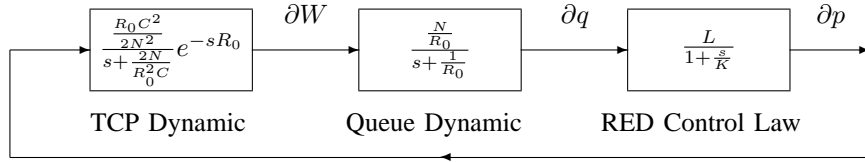


Fig. 1. Block diagram of linearized RED control system

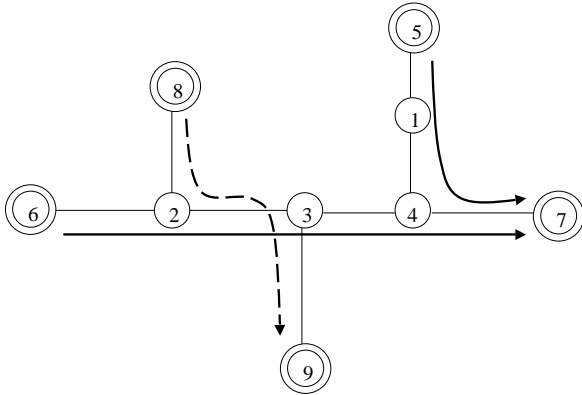


Fig. 2. Network topology

TABLE I  
NETWORK PARAMETERS

Link	Capacity (Mbps)	Propagation Delay (ms)
1-4	20	15
2-3	10	5
3-4	20	10
4-7	10	10
5-1	20	15
6-2	20	5
8-2	20	15
3-9	20	10

The open-loop transfer function of the system in Figure 1 is:

$$F(s) = \frac{L \frac{(RC)^3}{(2N)^2} e^{-sR}}{\left(1 + \frac{s}{K}\right) \left(1 + \frac{s}{\frac{2N}{R^2 C}}\right) \left(1 + \frac{s}{R}\right)} \quad (5)$$

In [9] the authors present RED configuration rules, that guarantee the stability of the linear feedback control system in Figure 1 for  $N \geq N^-$  and  $R_0 \leq R^+$ .

### III. AN INSTABILITY EXAMPLE

We consider a parking lot network whose topology is depicted in Figure 2. The capacity and the propagation delay of each link are reported in Table I. Packet size is 1500 bytes. Links between nodes 4 and 7 and between nodes 2 and 3 will play the role of bottlenecks.

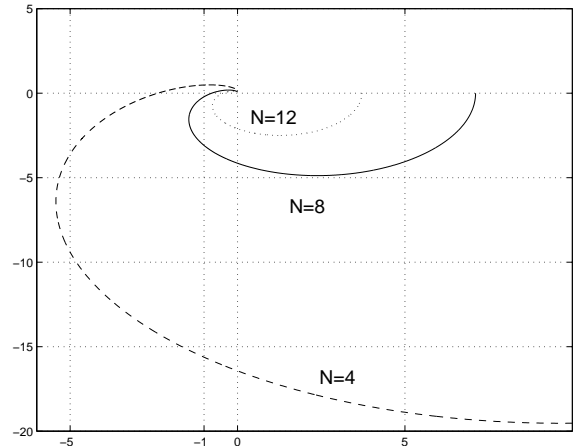


Fig. 3. Nyquist plots for the considered RED configuration and  $N = 4, 8, 12$  flows

The RED algorithm is deployed at nodes 4 and 2, respectively to manage the output queues for the link 4 – 7 and 2 – 3. In what follows we refer to these buffers simply as node 4 buffer and node 2 buffer, without specifying the link, or as queue 4 ( $q_4$ ) and queue 2 ( $q_2$ ).

Our RED configuration relies on the control theoretic analysis of RED presented in [9]. Nevertheless, we do not adopt exactly the configuration rules proposed there, since their high stability margins do not allow simple counter-example, but we use common thumb rules and then we verify RED-configuration stability through the Nyquist plot of the open loop transfer function.

We recall that the Nyquist criterion allows one to study the stability of the closed loop system through the polar plot of the open loop transfer function  $F(j\omega)$ . For the functions we are interested in, the closed loop system is stable if and only if the plot does not encircle the point  $(-1, 0)$ .

We choose  $THR_{min} = 2$ ,  $THR_{max} = 20$ ,  $P_{max} = 5\%$ , and  $w_q = 0.002$ . This configuration guarantees stability if the number of flows is greater than or equal to  $N^- = 7$  and the Round Trip Time is lower than or equal to  $110ms$ . Figure 3 shows the Nyquist plot of the open loop transfer function (5) for  $R = 110ms$  and different number of flows  $N$ .

Simulations were conducted through ns v2.1b9a [12]. We

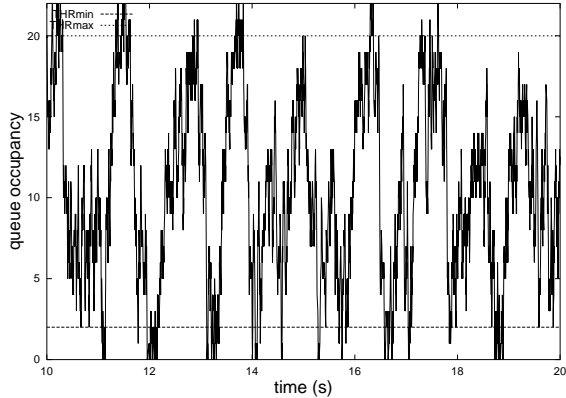


Fig. 4. Instantaneous buffer occupancy with number of flows  $N = 8$

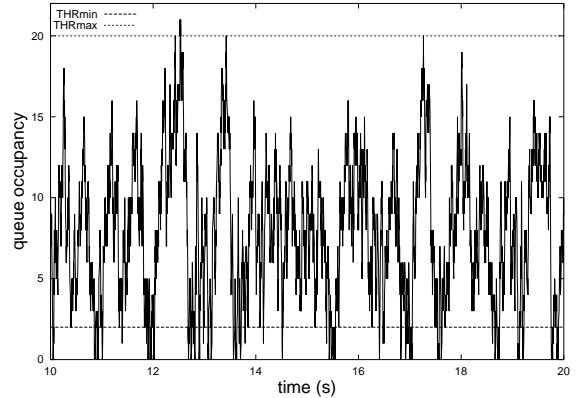


Fig. 5. Instantaneous buffer occupancy with  $N = 6$

used TCP Reno implementation.

### A. Single Bottleneck

A primary question is which metric is particularly suitable to catch instability phenomena. In this sense, though instability is by many authors addressed looking at the amplitude of queue size oscillations, we will better refer to the normalized standard deviation as a more suitable metric to analyze instability phenomena. For example, when the number of flows decreases, stability margins decrease according to the linear model developed in [9], and one could expect larger queue oscillations. Yet, at the same time the queue average value decreases and the physical constraint of positive queue values can determine smaller oscillations. Ultimately, the cause is the RED coupling of queue length and loss probability, which lets the operating point depend from the network conditions, like the load level. From a control theoretic point of view one says that the RED controller has steady state regulation errors.

Now, in order to analytically show how instability of the linear model concretely affects the network performance, we first present some results regarding the single bottleneck scenario.

Two aggregates, each one of four TCP flows ( $N = 8$ ), enter the network through node 5 and node 6 with destination node 7 (solid lines in figure 2). The link between nodes 4 and 7 is congested.

Figure 4 shows the instantaneous queue occupancy time-plot for the buffer at node 4. RED should be able to keep the queue occupancy within the two thresholds (dotted lines).

Let us progressively reduce the number of flows through the network and see if instability occurs as claimed in [9]. In Figure 5 the buffer occupancy is shown to revisit with a higher frequency the regions associated to buffer overload and underload (out of RED thresholds).

Numerical results for the throughput and the normalized standard deviation are shown in Table II. As the total flow number decrease from 8 to 6 we note that i) the throughput over the link 4 – 3 reduces from 9.80 Mbps to 9.70 Mbps, ii) both the average queue occupancy and the oscillation

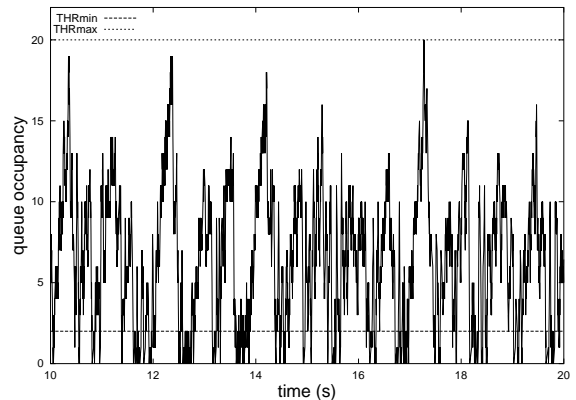


Fig. 6. Instantaneous buffer occupancy with  $N = 4$

amplitude decrease, respectively from 10.0 to 8.19 and from 5.26 to 4.64, and iii) the normalized standard deviation, i.e. the ratio between standard deviation and mean, increases from 0.52 to 0.56.

If we reduce drastically the number of flows to 4, the above RED configuration, turns to be too aggressive, which is evidenced by higher frequencies of buffer occupancy oscillations and further reduction of the throughput. Even longer periods, where buffer is underloaded results from Figure 6.

Experimental results show that instability predicted by the model in [9] leads to reduced link utilization and higher normalized oscillations (higher jitter in percentage).

Conversely, if we increase the number of flows, higher throughput and lower jitter can be achieved.

Node 2 buffer has the same RED configuration. Table II shows similar results when only the link 2 – 3 is congested, due to flows coming from nodes 6 and 8.

### B. Two Bottlenecks

We now draw the attention to the fact that buffer occupancy instability, may arise when flows through node 4 are in part already controlled by some other congested upstream

TABLE II  
NUMERICAL RESULTS

$N_6$	$N_5$	$N_8$	$Thr_6$	$Thr_5$	$Thr_8$	$queue_4$ occupancy	$queue_4$ oscillation	$queue_2$ occupancy	$queue_2$ oscillation
6	6	0	5.36	4.57	-	13.6	0.41	0.94	0.26
4	4	0	5.39	4.41	-	10.0	0.52	0.95	0.25
3	3	0	5.29	4.41	-	8.19	0.56	0.96	0.28
2	2	0	5.32	4.17	-	6.31	0.64	0.97	0.43
0	4	0	-	9.49	-	5.51	0.72	0	0
4	0	4	4.92	-	4.92	0	0	10.48	0.48
4	4	4	3.60	6.06	6.12	8.05	0.73	9.36	0.62
4	4	6	3.03	6.59	6.82	7.51	0.75	11.60	0.53
4	4	8	2.59	7.03	7.33	7.16	0.74	11.60	0.45

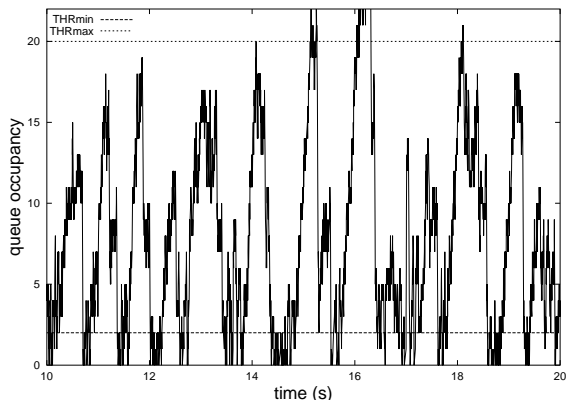


Fig. 7. Instantaneous node 4 buffer occupancy in a two bottleneck scenario

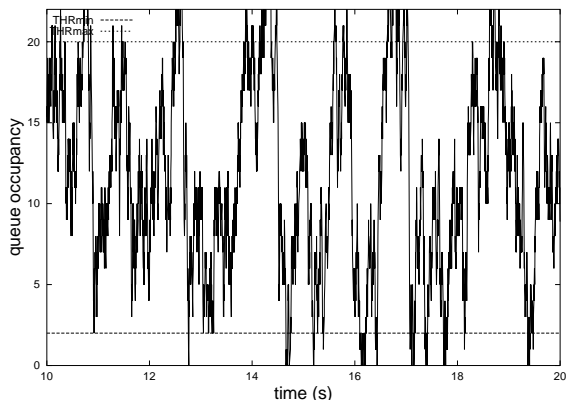


Fig. 8. Instantaneous node 2 buffer occupancy in a two bottleneck scenario

node, for instance, node 2 when link 2–3 is congested (see Figure 2).

To recreate artificially such a scenario, let us introduce an additional aggregate entering the network from node 8, with destination node 9 (dotted line in figure 2). Node 4 buffer occupancy for a 4-flows aggregate exhibits a high oscillatory behavior in figure 7.

From Figure 8 instability arises also at node 2.

The numerical values stored in the last three rows of Table II support quantitatively our claims rising from Figures 7

and 8. In particular the normalized oscillation values of node 4 buffer are comparable to the value stored in the fifth row, corresponding to a single bottleneck instability scenario due to a low number of flows ( $N_5 + N_6 = 4 < N^-$ ).

The normalized oscillation values in Table II confirm quantitatively the feelings obtained from Figures 7 and 8.

Note that, though the number of flows at each node and the flow round trip time should assure stable operation, instability arises due to the traffic aggregate from 6 to 7, which traverses both the congested links.

This example shows the limits of local AQM configuration ignoring the distributed nature of TCP flows control in a multiple bottleneck scenario. If we consider the configuration rules given in [9], instability probably does not arise in such a simple example, but there is a reduction of stability margins. This modifies the system dynamic response and reduces the system robustness to the flows number and the round trip time variation.

#### IV. THE ANALYTICAL INSIGHT

In this section, we provide an insight into the physical causes of instability in our counter-example. We start from a nonlinear two bottleneck model of the network with some simplifying assumptions, and prove that the system is unstable. Then, we come back to single bottleneck systems, by considering only one TCP aggregate at a time, the other ones acting as non reactive flows. Despite such system decoupling is not correct from an analytical point of view, it allows us to get again the linear system described in Section II, but with some different parameters. Hence, the effect of multiple bottlenecks can be helpfully seen as a parameter variation in the same single bottleneck model we considered to configure the RED. It allows us to understand why instability arises and to simply predict the effect of some network scenario changes, such as the number of flows and the propagation delays. The limits of such an approximation are detailed in the following subsection.

##### A. Two Bottleneck Model

We extend the single bottleneck congestion model described in Section II to the case of two congested nodes. With reference to the network topology depicted in Figure 2 we obtain

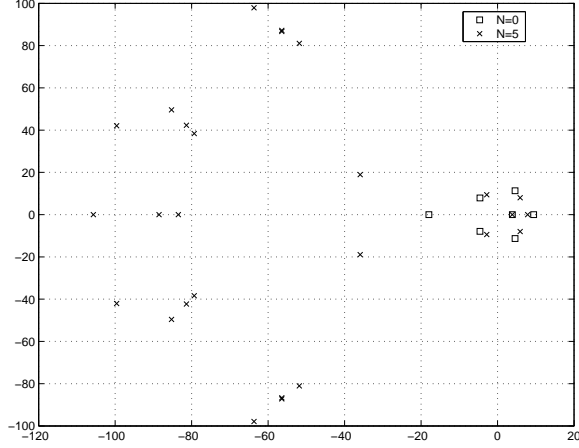


Fig. 9. Poles of the two bottleneck system with two Padé approximations of time delays

$$\begin{cases} \dot{W}_5 = \frac{1}{R_5} - \frac{W_5 W_5(t-R_5)}{2R_5(t-R_5)} p_4(t-R_5) \\ \dot{W}_6 = \frac{1}{R_6} - \frac{W_6 W_6(t-R_6)}{2R_6(t-R_6)} (p_2(t-R_6) + \\ \quad + p_4(t-R_6) - p_2(t-R_6)p_4(t-R_6)) \\ \dot{W}_8 = \frac{1}{R_8} - \frac{W_8 W_8(t-R_8)}{2R_8(t-R_8)} p_2(t-R_8) \\ \dot{q}_4 = \frac{W_5}{R_5} N_5 + \frac{W_6}{R_6} N_6 - 1_{q_4} C_4 \\ \dot{q}_2 = \frac{W_6}{R_6} N_6 + \frac{W_8}{R_8} N_8 - 1_{q_2} C_2 \end{cases} \quad (6)$$

where  $R_5 = T_{p2} + \frac{q_4}{C_4}$ ,  $R_8 = T_{p1} + \frac{q_2}{C_2}$ ,  $R_6 = T_{p1} + \frac{q_2}{C_2} + \frac{q_4}{C_4}$ . For sake of simplicity in (6), the time dependance is indicated only for delayed functions.

The above model relies essentially on the assumptions of the original single bottleneck model. One further limit is the way node 6 traffic has been considered in queue 4 equation: this equation ignores i) the delay from queue 2 to queue 4, and ii) that this traffic comes from another congested node, and therefore has been shaped by queue 2 (the outgoing traffic cannot overcome  $C_2$ ).

By linearizing the equation system 6 and using Padé functions to approximate time-delays, we obtain a rational Linear Time Invariant model. Thus, we study system stability considering the poles. Figure 9 shows the system poles for two different Padé approximations. The zero-order approximation ( $N = 0$ ) simply corresponds to neglecting time-delays ( $e^{-sR} \simeq 1$ ). There are four poles with positive real part, hence the system is unstable. As the approximation order increases, the number of poles increases, and, at least up to the 20th order approximation, there are always four poles with positive real part. For example poles for the fifth order approximation are shown in Figure 9.

### B. Decoupling into three single bottleneck models

Now, we consider individually each of the three aggregates and assume the other flows are non reactive ones, i.e., we focus on  $W_i$ , and assume  $W_j/R_j = W_{j0}/R_{j0} = \text{cost}$ , for  $j \neq i$ . Due to congestion at nodes 2 and 4,

$N_5 W_{50}/R_{50} + N_6 W_{60}/R_{60} \simeq C_4 = C_2 \simeq N_8 W_{80}/R_{80} + N_6 W_{60}/R_{60}$ . We can derive the following models for the aggregates 5 and 8 ( $(i, j) = (5, 4)$  and  $(i, j) = (8, 2)$  respectively):

$$\begin{cases} \dot{W}_i = \frac{1}{R_i} - \frac{W_i W_i(t-R_i)}{2R_i(t-R_i)} p_j(t-R_i) \\ \dot{q}_j = \frac{W_i}{R_i} N_i + \frac{W_{60}}{R_{60}} N_6 - 1_{q_j} C_j, \end{cases} \quad (7)$$

and the following model for aggregate 6:

$$\begin{cases} \dot{W}_6 = \frac{1}{R_6} - \frac{W_6 W_6(t-R_6)}{2R_6(t-R_6)} (p_2(t-R_6) + \\ \quad + p_4(t-R_6) - p_2(t-R_6)p_4(t-R_6)) \\ \dot{q}_4 = \frac{W_{50}}{R_{50}} N_5 + \frac{W_6}{R_6} N_6 - 1_{q_4} C_4 \\ \dot{q}_2 = \frac{W_6}{R_6} N_6 + \frac{W_{80}}{R_{80}} N_8 - 1_{q_2} C_2. \end{cases} \quad (8)$$

The equation system (7) is the same as in the previous single bottleneck system: bottleneck capacities are respectively equal to  $C_5^{eq} = C_4 - N_6 W_{60}/R_{60} = N_5 W_{50}/R_{50}$  for aggregate 5 and  $C_8^{eq} = C_2 - N_6 W_{60}/R_{60} = N_8 W_{80}/R_{80}$  for aggregate 8.

Neglecting the product  $p_2 p_4$  in comparison to the terms  $p_2$  and  $p_4$ , the equation system (8) reduces to the single bottleneck model too, where the bottleneck capacity is  $C_6^{eq} = C_4 - N_5 W_{50}/R_{50} = C_2 - N_8 W_{80}/R_{80} = N_6 W_{60}/R_{60}$  and we can consider a single RED queue where  $P_{max}^{eq} = 2P_{max}$ .

The previous results are quite intuitive. Nevertheless, we can obtain them via linearization of the equation systems 7 and 8 (similarly to Appendix I of [9]). Thus, we obtain the following open-loop transfer function:

$$F_i(s) = \frac{L_i^{eq} \frac{(R_{i0} C_i^{eq})^3}{(2N_i)^2} e^{-sR_{i0}}}{\left(1 + \frac{s}{K}\right) \left(1 + \frac{s}{\frac{2N_i}{R_{i0}^2 C_i^{eq}}}\right) \left(1 + \frac{s}{\frac{1}{R_{i0}}}\right)} \quad (9)$$

where  $i = 5, 6, 8$ .  $L_i^{eq} = 2L$  for  $i = 6$ ,  $L_i^{eq} = L$  for  $i = 5, 8$ . These transfer function differs from transfer function in (5), only for the parameter values.

### C. Stability considerations

In this section, we justify instability results shown in Section III, by applying the Nyquist criterion to the open-loop transfer function in (9).

We remember that our RED configuration assure stability for the system whose transfer loop function is (5) with  $N = 8$ ,  $R = 110\text{ms}$  and  $C = C_4 = C_2$ .

From the new open-loop transfer functions, we see that the decrease of the number of effective flows for all the three aggregates and the increase of the RED slope for the aggregate 6 contribute to system instability. Yet, the decrease of the equivalent capacity makes the system more stable. In order to evaluate the dominating effect we have to consider numerical values for the parameters, but we can state that as the number of flows  $N_8$  increases,  $W_5$  exhibits instability. As the number of flows  $N_8$  increase, the aggregate 6 is going to be harder choked, hence  $C_{5eq}$

approaches  $C_4$  and the Nyquist plot corresponding to the transfer function (9) approaches the dashed curve in Figure 3, which corresponds to  $N = 4$ ; the plot encircles the point  $(-1, 0)$  and the corresponding closed loop system is unstable.

With the numerical values from Table II, the single bottleneck models predict that  $W_5$  is unstable, whereas  $W_6$  and  $W_8$  are stable:  $W_8$  is stable due to smaller RTT in comparison to aggregate 5 ( $T_{p1} \leq T_{p2}$ ); as regards the window size  $W_6$  a smaller  $C_{6eq}$  compensates the  $N$  reduction and  $L$  increase.

As regards the instability of the multiple bottleneck system, all the variables show instability. As a matter of fact,  $W_5$  instability implies the  $q_4$  oscillations and hence the  $p_4$  oscillations. The last affect the throughput of the aggregate 6. Aggregate 6 couples the two queues and hence it yields instability to  $q_2$ , and so on.

Single bottleneck models allows us to simply predict for example the effect of increasing  $N_8$ . We have already stated that  $W_5$  instability increases, at the same time  $W_8$  becomes more stable and the coupling between the two queues by the aggregate 6 reduces. Hence, we expect an overall more stable behavior at queue 2. Performance metrics in Table II for  $N_8 = 6$  and  $N_8 = 8$  confirm results of single bottleneck models: instability increases at the downstream node and it decreases at the upstream one.

As regards the validity of our simple analysis, let us consider for example  $W_5$ . Results from System 7 are more accurate as long as i) aggregate 6 is small ( $W_6(t) \ll W_5(t)$ ), or ii) it is not small, but it is not markedly affected by the dynamics of the aggregate 5 and of the queue 4, i.e. as long as the behavior of the aggregate 6 is determined elsewhere, in our example at the congested node 2. For example the model provides better a approximation if the number of flows  $N_8$  increases or the round trip time  $R_8$  decreases.

## V. CONCLUSIONS AND FUTURE WORK

In this paper we showed that RED configuration based on a single-bottleneck assumption may not prevent from traffic instability when congestion occurs, at the same time, in two different locations of the network.

This suggests that the effect of multiple bottlenecks could be counteracted by robust configuration of AQM controllers. In particular the minimum number of flows  $N^-$  should not take into account flows being controlled by other nodes. Hence the network administrator should evaluate not only the minimum number of flows at each node and their round trip time, but he should also get more sophisticated information about traffic matrix across the network and contemporaneously congested nodes.

Another approach would be to implement new cooperative AQM controllers, that base their control action on information about the congestion status of the other nodes. Simplicity is an obvious requirement, particularly for signalling among nodes.

We think that the Explicit Congestion Notification (ECN) field [13] in IP packets could be usefully employed for inter-nodes signalling. ECN has been proposed as a light in-band signalling form between nodes and client, but it appears to be a simple way for nodes to transmit downstream information about their congestion status. The advantages of ECN employment are: no further network transmission resources are required, information travels along the data path, and it can be used by all the nodes controlling the flow.

AQM controller should monitor the ingoing traffic, evaluate the share of traffic controlled elsewhere, by the percentage of packets with the Congestion Experienced codepoint set (CE packets) and set some tunable parameters according to the controlled traffic share. For example a RED controller could decrease the dropping curve slope  $L$  as the percentage of CE packets increases in order to maintain a stable operation.

## REFERENCES

- [1] B. Braden, D. Clark, J. Crowcroft, B. Davie, S. Deering, D. Estrin, S. Floyd, V. Jacobson, G. Minshall, C. Partridge, L. Peterson, K. Ramakrishnan, S. Shenker, J. Wroclawski, and L. Zhang, Recommendations on queue management and congestion avoidance in the internet, RFC 2309, April 1998.
- [2] S. Floyd, V. Jacobson, "Random Early Detection Gateways for Congestion Avoidance", IEEE ACM Transactions on Networking, 1993.
- [3] S. Floyd, R. Gummadi, S. Shenker, "Adaptive RED: An Algorithm for Increasing the Robustness of RED's Active Queue Management", technical report available at <http://www.icir.org/floyd/papers/adaptiveRed.pdf>, August, 2001.
- [4] S. Athuraliya, V. H. Li, S. H. Low and Q. Yin, "REM: Active Queue Management", IEEE Network, May 2001
- [5] W. Feng, D. Kandlur, D. Saha, K. Shin, "Blue: A New Class of Active Queue Management Algorithms", UM CSE-TR-387-99, 1999
- [6] M. Christiansen, K. Jeffay, D. Ott, F.D. Smith, Tuning RED for web traffic, in Proceedings of ACM/SIGCOMM, 2000.
- [7] M. May, T. Bonald, J. C. Bolot, Analytic Evaluation of RED Performance, in Proceedings of IEEE/INFOCOM, 2000.
- [8] V. Firoiu, M. Borden, A Study of Active Queue Management for Congestion Control, in Proceedings of IEEE/INFOCOM, 2000.
- [9] C. V. Hollot, V. Misra, D. Towsley, W. Gong "A Control Theoretic Analysis of RED" *IEEE INFOCOM*, 2001.
- [10] V. Misra, W. Gong, D. Towsley, Fluid-based Analysis of a Network of AQM Routers Supporting TCP Flows with an Application to RED, in Proceedings of ACM/SIGCOMM, 2000.
- [11] C. V. Hollot, V. Misra, D. Towsley, W.-B Gong "Analysis and Design of Controllers for AQM Routers supporting TCP Flows" *IEEE ACM Trans on Automatic Control*, pp., vol.47, no.6, 2002.
- [12] Network Simulator <http://www.isi.edu/nsnam/ns/>
- [13] The Addition of Explicit Congestion Notification (ECN) to IP. Ramakrishnan, K.K., Floyd, S., and Black, D. RFC 3168, Proposed Standard, September 2001